Circular RNA 0000096 affects cell growth and migration in gastric cancer

Peifei Li[1,3], Huilin Chen[2], Shengcan Chen[1], Xiaoyan Mo[1], Tianwen Li[1], Bingxiu Xiao[1], Rui Yu[1] and Junming Guo*,[1]

[1]Department of Biochemistry and Molecular Biology, Zhejiang Key Laboratory of Pathophysiology, Ningbo University School of Medicine, Ningbo 315211, China and [2]Department of Human Body Function, Ningbo College of Health Sciences, Ningbo 315010, China

Background: Circular RNAs (circRNAs) are a class of non-coding RNAs broadly expressed in cells of various species. Their role in cancers, especially in gastric cancer, is poorly understood.

Methods: Circular RNA 0000096 (hsa_circ_0000096) levels in 101 paired gastric cancer tissues and adjacent non-tumorous tissues from patients with gastric cancer were detected by real-time quantitative reverse transcription-polymerase chain reaction. A receiver operating characteristic curve was generated to evaluate the diagnostic value of hsa_circ_0000096. RNA interference was used to manipulate the expression of hsa_circ_0000096. Its biological effects were evaluated by flow cytometry, real-time cell analysis, a wound scratch assay, western blot analysis and xenograft models.

Results: Hsa_circ_0000096 was found to be significantly downregulated in gastric cancer tissues and gastric cancer cell lines compared with paired adjacent non-tumorous tissues and normal gastric epithelial cells ($P<0.001$). Moreover, knockdown of hsa_circ_0000096 significantly inhibited cell proliferation and migration *in vitro* and *in vivo*. The results of both immunohistochemical and western blot analyses showed that the protein levels of cyclin D1, cyclin-dependent kinase 6 (CDK6), matrix metalloproteinase-2 and MMP-9 were significantly reduced *in vitro* and *in vivo*. A gastric cancer xenograft nude mouse model indicated that Ki67 and VEGF were reduced in a dose-dependent manner following knockdown of hsa_circ_0000096. However, the expression of E-cadherin increased.

Conclusions: Hsa_circ_0000096 may be used as a potential novel biomarker for gastric cancer. It affects gastric cancer cell growth and migration by regulating cyclin D1, CDK6, MMP-2 and MMP-9.

Gastric cancer is one of the most common human cancers (Li *et al*, 2016). Early- and late-stage diagnosis and treatment of gastric cancer have very different outcomes. The 5-year survival rate of early gastric cancer can reach 90–95%. However, if gastric cancer develops to a late stage, the mortality rate is greatly increased. Thus, it is very important to diagnose gastric cancer early. For this reason, effective, stable and ideal molecular diagnostic markers of gastric cancer must be identified.

Compared with microRNAs (miRNAs) and long non-coding RNAs (lncRNAs) that have been more deeply studied, circular RNAs (circRNAs), as novel non-coding RNAs (Hansen *et al*, 2013; Memczak *et al*, 2013), are more stable in plasma and gastric juice (Li *et al*, 2015). This remarkable feature makes them an ideal choice for use as molecular markers of gastric cancer. However, the biological functions of circRNAs in human diseases, especially in cancer, are unclear. Therefore, this study identified the value of circRNAs in the diagnosis of gastric cancer and their biological roles in the occurrences of gastric cancer.

In this study, based on circRNA databases (Ghosal *et al*, 2013; Glažar *et al*, 2014), we focused on hsa_circ_0000096 (Aliashsa_

circ_001013). Its gene is located at chr1:100515464-100535241. The spliced sequence length is 807 nt, and its gene symbol is HIAT1. Our results showed that hsa_circ_0000096 was downregulated in gastric cancer tissues and cells. Further study showed that by suppressing the expression levels of cyclin D1, cyclin-dependent kinase (CDK) 6, matrix metalloproteinase (MMP)-2, and MMP-9, hsa_circ_0000096 affected gastric cancer cell proliferation and migration. A xenograft nude mouse model further confirmed the tumour-suppressive activity of hsa_circ_0000096.

MATERIALS AND METHODS

Tissue samples. All gastric cancer tissues were collected from surgical specimens at the Affiliated Hospital of Ningbo University School of Medicine, China. The specimens were confirmed by pathological examination. The Human Research Ethics Committee of Ningbo University approved all aspects of the protocols. Written informed consent was obtained from all subjects.

Cell culture. Five human gastric cancer cell lines, AGS, BGC-823, HGC-27, SGC-7901 and MGC-803, were obtained from the Shanghai Institutes for Biological Sciences, Chinese Academy of Sciences (Shanghai, China). The human gastric epithelial cell line GES-1 was obtained from the Cancer Institute and Hospital of the Chinese Academy of Medical Sciences (Beijing, China). All cell lines were grown in RPMI Medium 1640 (Life Technologies, Carlsbad, CA, USA) plus 10% fetal bovine serum (FBS) at 37 °C in a humidified atmosphere with 5% CO_2. The cells were counted using a TC10 Automated Cell Counter (Bio-Rad, Hercules, CA, USA).

RNA extraction. Both RNA from tissues and cells were extracted using TRIzol Reagent (Invitrogen, Karlsruhe, Germany) according to the manufacturer's protocol. The RNA quantity was measured with a SmartSpec Plus spectrophotometer (Bio-Rad). The RNA purity was evaluated according to the A_{260}/A_{280} ratio.

qRT–PCR analysis. Real-time quantitative reverse transcription-polymerase chain reaction (qRT–PCR) of hsa_circ_0000096 was performed using a GoTaq 2-Step RT–qPCR System (Promega, Madison, WI, USA) in an Mx3005P QPCR System (Stratagene, La Jolla, CA, USA) according to the manufacturer's protocol. According to our previous report (Li et al, 2015), the use of divergent primers can amplify the circRNA, but not the linear RNA; the use of convergent primers can amplify the linear RNA but not the circRNA. The sequences of hsa_circ_0000096 divergent primers were as follows: 5′-CAGTCCTTGGCATTCTTTCC-3′ and 5′-GTGGGTGCTGTCAATAGTCC-3′. The sequences of glyceraldehyde 3-phosphate dehydrogenase (GAPDH) convergent primers were as follows: forward, 5′-TCGACAGTCAGCCGCATCTTCTTT-3′; reverse, 5′-ACCAAATCCGTTGACTCCGACCTT-3′. GAPDH was used as a control. qRT–PCR of miRNAs was performed using miScript II RT Kits (Qiagen, Hilden, Germany), miScript SYBR Green PCR Kits (Qiagen) and miScript Primer Assays (miR-200a-3p primer, miR-224-5p and RNU6-2 primer; Qiagen) in an Mx3005P QPCR System (Stratagene) according to the manufacturer's protocol. RNU6-2 was used as a qRT–PCR control for miRNAs.

All experiments were performed in triplicate. Relative quantification of gene expression was performed by the $2^{-\Delta\Delta Ct}$ method (Shao et al, 2014; Xia et al, 2015).

Transient transfection. For the transfection of small interfering RNAs (siRNAs), GES-1, AGS, BGC-823, HGC-27, SGC-7901 and MGC-803 cells (2×10^5) were seeded in six-well plates. The following day, cells were transfected with 100 nM of siRNA using Lipofectamine 2000 Reagent (Life Technologies). The sequences of the three hsa_circ_0000096 siRNA were 5′-CAUUAUUGCAC

AGCCUCAATT-3′ (sense) and 5′-GUAAUAACGUGUCGGAG UUTT-3′ (antisense), 5′-GUGUCUAUCAUGCAGUUAUTT-3′ (sense) and 5′-AUAACUGCAUGAUAGACACTT-3′ (antisense), 5′-CUUGGUGGGUAUUACAUGAATT′ (sense) and 5′-UUCAUG UAAUACCACCAAGTT-3′ (antisense). The sequences of the negative control siRNAs were 5′-UUCUCCGAACGUGUCACG UTT-3′ (sense) and 5′-ACGUGACACGUUCGGAGAATT-3′ (antisense). The siRNAs were synthesised by GenePharma Co., Ltd. (Shanghai, China).

Western blot. Cells were collected and lysed with cell lysis buffer for western blotting (Beyotime, Haimen, China). The proteins (30 μg per lane) were separated on 12% SDS-polyacrylamide gels and transferred on a polyvinylidene fluoride membrane (Millipore, Billerica, MA, USA). Immunoblotting of the membrane was performed using the following primary antibodies: anti-CDK6 (Boster, Wuhan, China), anti-cyclin D1 (Affinity, Cincinnati, OH, USA), anti-MMP-2 (Boster), anti-MMP-9 (Boster) and anti-β-actin (4 A Biotech, Beijing, China). The signals were revealed after incubation with the recommended secondary antibodies using an Odyssey Infrared Imaging System (LI-COR, Lincoln, NE, USA). β-actin was used as the control.

Cell cycle analysis. The cells were washed in phosphate-buffered saline (PBS) and fixed in 75% ice-cold ethanol at − 20 °C overnight. After rehydration with ice-cold PBS, cells were stained with PI/RNase Staining Buffer (BD Biosciences, San Jose, CA, USA) and analysed using flow cytometry on a FACSCalibur Flow Cytometer (BD Biosciences) using the CellQuest Pro software (BD Biosciences).

Cell apoptosis analysis. Cells were washed in RPMI Medium 1640 plus 10% FBS and cells were resuspended with a binding buffer. Cells were incubated on ice for 5 min after adding propidium iodide and Annexin V under dark conditions, and then analysed by flow cytometry on a FACSCalibur Flow Cytometer (BD Biosciences) using the CellQuest Pro software.

Cell proliferation assay. The proliferation assay was performed in an E-Plate 96 using a Real-Time Cell Analyzer (ACEA Biosciences, San Diego, CA, USA) according to the manufacturer's protocol.

Cell migration assay. After scratching (recorded as 0 h), cells were incubated with serum-free medium for 24 h. The Image pro plus 6.0 software (Media Cybernetics Inc., MD, USA) was used to measure the distance at 0 and 24 h, and GraphPad Prism5 (GraphPad Software Inc., CA, USA) was used for statistical analysis.

Xenograft nude mouse model. Male BALB/c nude mice aged 6 weeks were purchased from Slac Laboratory Animal Center (Shanghai, China) and maintained under specific pathogen-free conditions in the animal care facility at Ningbo University. BGC-823 and MGC-803 cells (3×10^6 per 100 μl) transfected with siRNAs were subcutaneously injected into the back of nude mice, respectively. The tumour size was measured every other day. All procedures were monitored in accordance with the ethical standards and the care of animal and licensing guidelines, issued by the administrative government, under the protocol approved by the Committee on Animal Welfare of Ningbo University.

Tissue preparation and histological analysis. To determine the morphological alterations in tumour tissues, haematoxylin and eosin staining was carried out. The tumours were removed from the mice, cut into an appropriate size and fixed in 4% paraformaldehyde for 24 h. Subsequently, the specimens were placed in graded ethanol for dehydration, embedded in paraffin and cut at a thickness of 4 μm. The sections were deparaffinised, rehydrated and immersed in Mayer's haematoxylin for 5–10 min. After being washed with deionised water, the sections were dipped in 0.1% acid water, immersed in 1% eosin for 5 min for colour

development and washed with deionised water. Finally, the sections were run through an ascending alcohol series, cleared in xylene and mounted in Permount (Yanjing, Shanghai, China).

Immunohistochemical analysis. According to the manufacturer's instructions, the tumour tissues were first dewaxed and rehydrated using xylene and ethanol. Then, high-pressure heat was used for antigen retrieval. Next, anti-CDK6, anti-cyclin D1, anti-MMP-2, anti-MMP-9, anti-Ki67 (Proteintech, Wuhan, China), anti-VEGF (Boster) and anti-E-cadherin (CST, Danvers, MA, USA) were added, respectively. Finally, all sections were dehydrated, cleared, mounted and visualised with a diaminobenzidine-based colorimetric method and analysed with the Image Pro Plus 6.0 software (Media Cybernetics Inc.). The immunohistochemistry (IHC) index was defined as the average integral optical density.

Statistical analysis. The data are presented as the mean ± s.d. The differences between groups were evaluated with two-tailed Student's t-tests using the SPSS Statistics 20.0 software (IBM, Armonk, NY, USA). $P < 0.05$ was considered statistically significant.

RESULTS

Hsa_circ_0000096 was downregulated in gastric cancer. In this study, we first found that hsa_circ_0000096 was downregulated in gastric cancer (Figure 1A). Then, we further found that its levels in five human gastric cancer cell lines, AGS, BGC-823, HGC-27, SGC-7901 and MGC-803, were lower than the levels in the GES-1 human normal gastric epithelial cell line (Figure 1B).

Furthermore, we found that the cutoff value of hsa_circ_0000096 was 12.9 (Figure 1C). The area under the receiver operating characteristic curve (AUC) was 0.82 (Figure 1D). As our previous work revealed that hsa_circ_002059 was a potential biomarker for gastric cancer (Li et al, 2015), we wanted to investigate the combinative use of hsa_circ_0000096 and hsa_circ_002509. We found that the AUC was increased to 0.91 with the combination of hsa_circ_0000096 and hsa_circ_002509 (Figure 1D). These results suggested that hsa_circ_0000096 may be a potential biomarker for the screening of gastric cancer.

The clinical diagnostic value of hsa_circ_0000096 in gastric cancer. Considering the clinical pathological parameters of
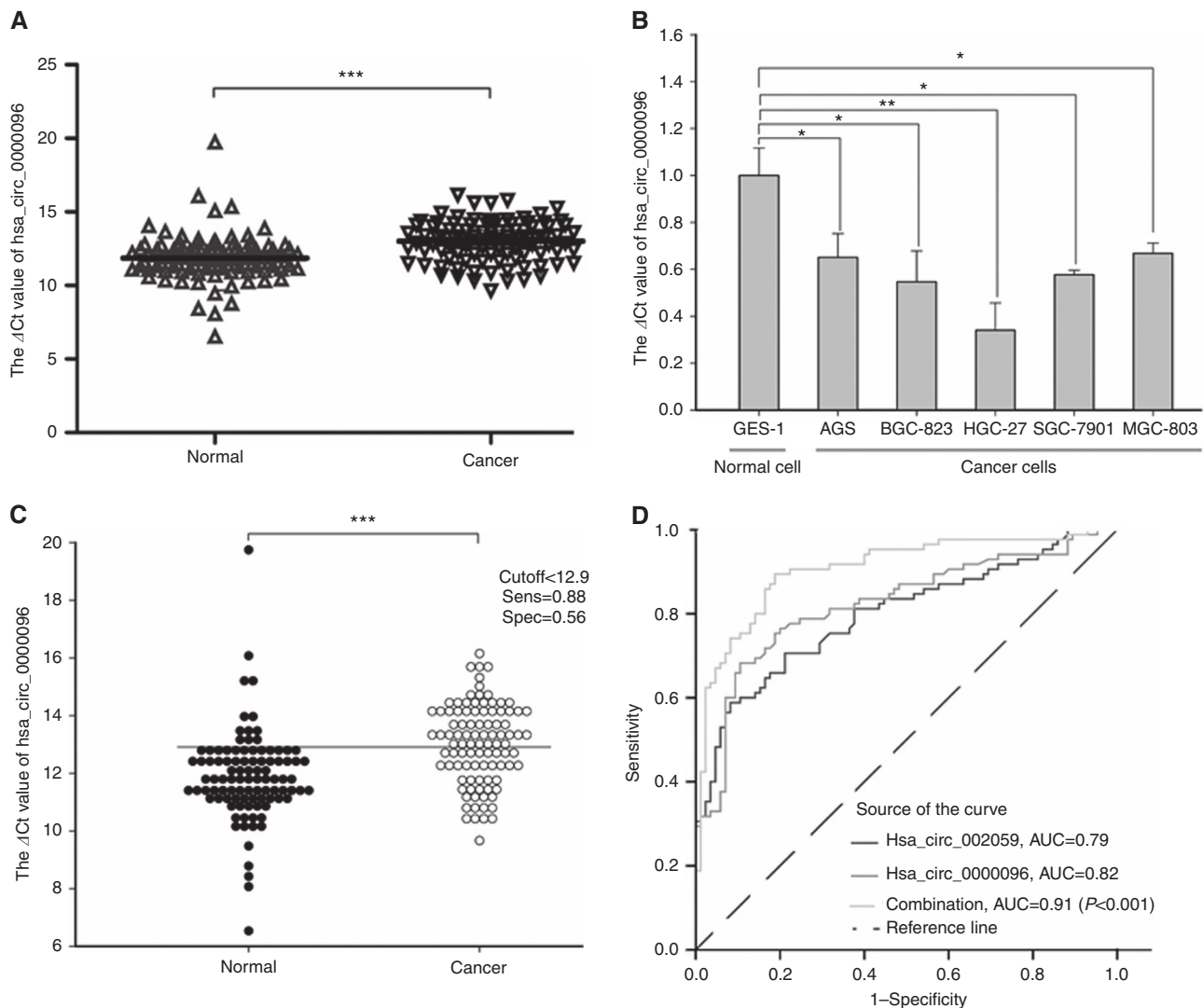

Figure 1. The diagnostic value of hsa_circ_0000096 in gastric cancer. The expression of hsa_circ_0000096 was downregulated in gastric cancer tissues (A) and gastric cancer cells (B). The cutoff of hsa_circ_0000096 was 12.9 (C) and the area under the receiver operating characteristic (ROC) curve (AUC) was 0.82 (D). Data are presented as the mean ± s.d., $n = 3$. *$P < 0.05$, **$P < 0.01$, ***$P < 0.001$.

patients with gastric cancer, we found that the aberrant expression of hsa_circ_0000096 was associated with several clinical pathological features such as gender ($P = 0.001$), invasion ($P = 0.046$) and TNM stage ($P = 0.024$; Supplementary Table 1). The majority of the patients were men, accounting for 74.3%. A total of 61.4% of invasion occurred at the T4 stage, and 59.4% patients were at III

and IV stages. However, we did not find any association between its expression levels and other clinicopathological factors (Supplementary Table 1).

Hsa_circ_0000096 regulates the cell cycle and cellular proliferation. The above results show that the expression level of
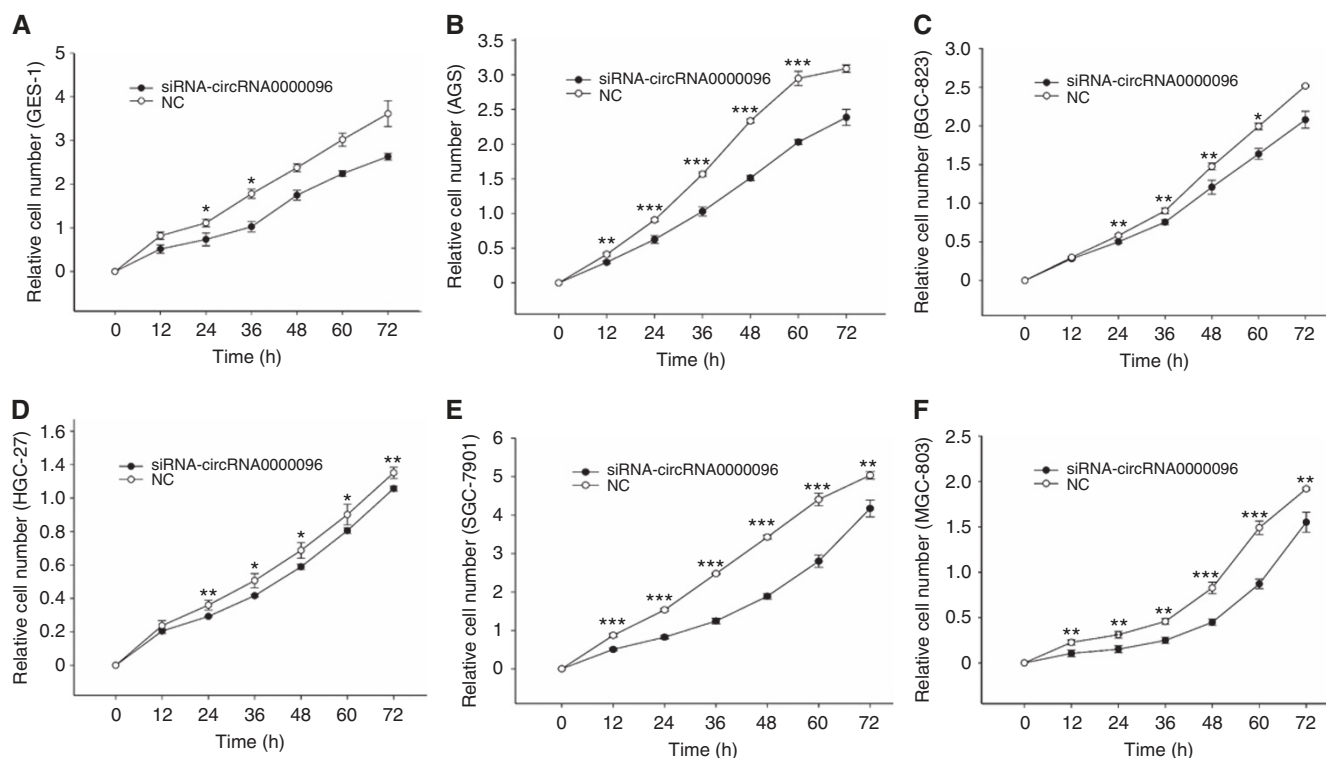

Figure 2. Knockdown of hsa_circ_0000096 inhibits cell proliferation. Growth curves of the human normal gastric epithelial cell line GES-1 (**A**) and the human gastric cancer cell lines AGS (**B**), BGC-823 (**C**), HGC-27 (**D**), SGC-7901 (**E**) and MGC-803 (**F**) following knockdown of hsa_circ_0000096. Data are presented as the mean ± s.d., $n = 3$. NC, negative control. $*P < 0.05$, $**P < 0.01$, $***P < 0.001$.
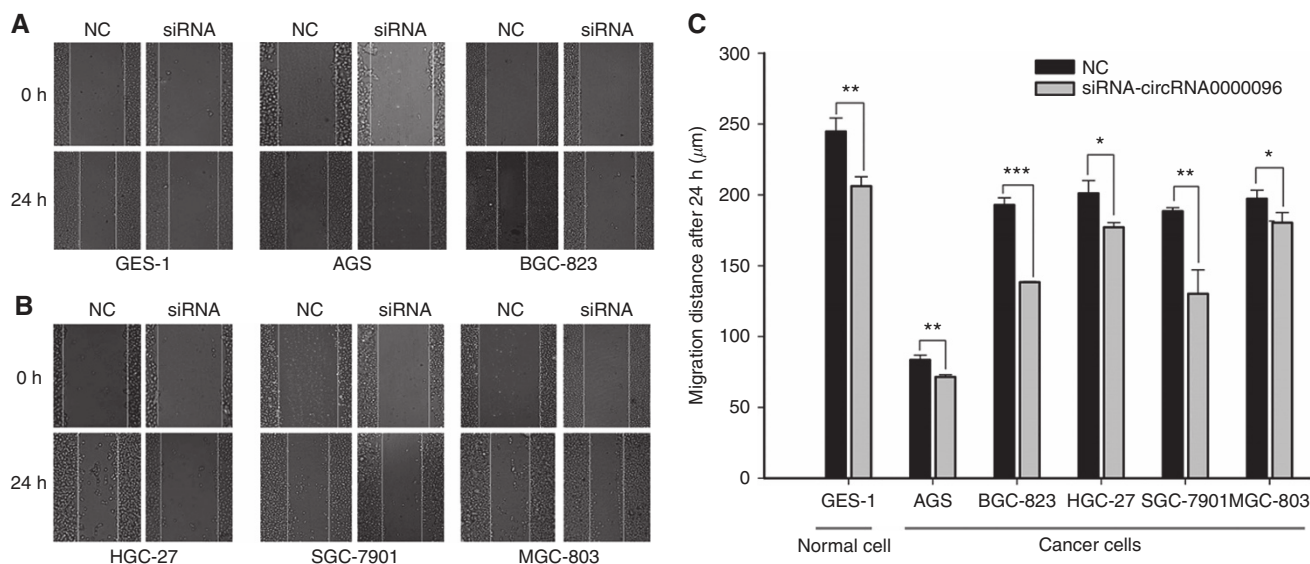

Figure 3. Knockdown of hsa_circ_0000096 reduces cell migration ability. Cell migration in a human normal gastric epithelial cell line and human gastric cancer cell lines following knockdown of hsa_circ_0000096 (**A**, **B**). Representative wound scratch assay results (**C**). Data are presented as the mean ± s.d., $n = 3$. NC, negative control. $*P < 0.05$, $**P < 0.01$, $***P < 0.001$.

hsa_circ_0000096 was downregulated in gastric cancer tissues and gastric cancer cell lines (Figure 1). Therefore, we decided to further investigate the effects of hsa_circ_0000096 on cell cycle, cell apoptosis and cell proliferation. Flow cytometry results demonstrated that knockdown of hsa_circ_0000096 by siRNAs blocked cell cycle progression and inhibited cells from the G_0/G_1 to S phase transition in GES-1, AGS, BGC-823, HGC-27, SGC-7901 and MGC-803 cells (Supplementary Figure 1). Moreover, knockdown of hsa_circ_0000096 also inhibited cell proliferation (Figure 2). However, no changes in apoptosis were found (Supplementary Figure 2).

Effects of hsa_circ_0000096 on cell migration. To further study the biological roles of hsa_circ_0000096, we used a wound scratch assay to analyse cell migration. The results clearly indicated that knockdown of hsa_circ_0000096 reduced the migration ability of the cells (Figure 3). The reduction in migration of the human gastric cancer cell line BGC-823 was the most pronounced, followed by MGC-803 cells.

Molecular mechanisms of hsa_circ_0000096 on cell proliferation and migration. To explore the molecular mechanisms of hsa_circ_0000096 on cell proliferation and migration, we used
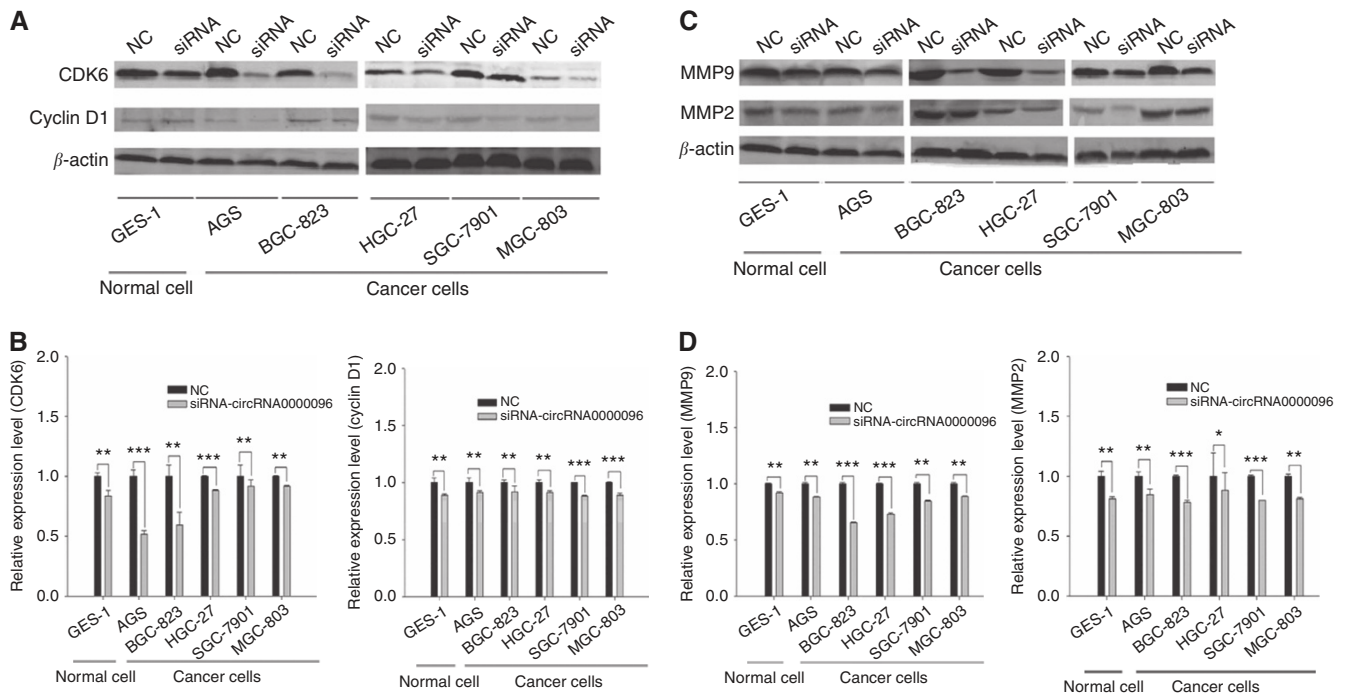

Figure 4. Expression levels of cell cycle-related and migration-related proteins in human normal gastric epithelial and human gastric cancer cell lines following knockdown of hsa_circ_0000096. Representative western blot results of cycle-related proteins cyclin D1 and CDK6 (**A**, **B**). Representative western blot results of migration-related proteins MMP-2 and MMP-9 (**C**, **D**). Data are presented as the mean ± s.d., $n = 3$. NC, negative control. *$P < 0.05$, **$P < 0.01$, ***$P < 0.001$.
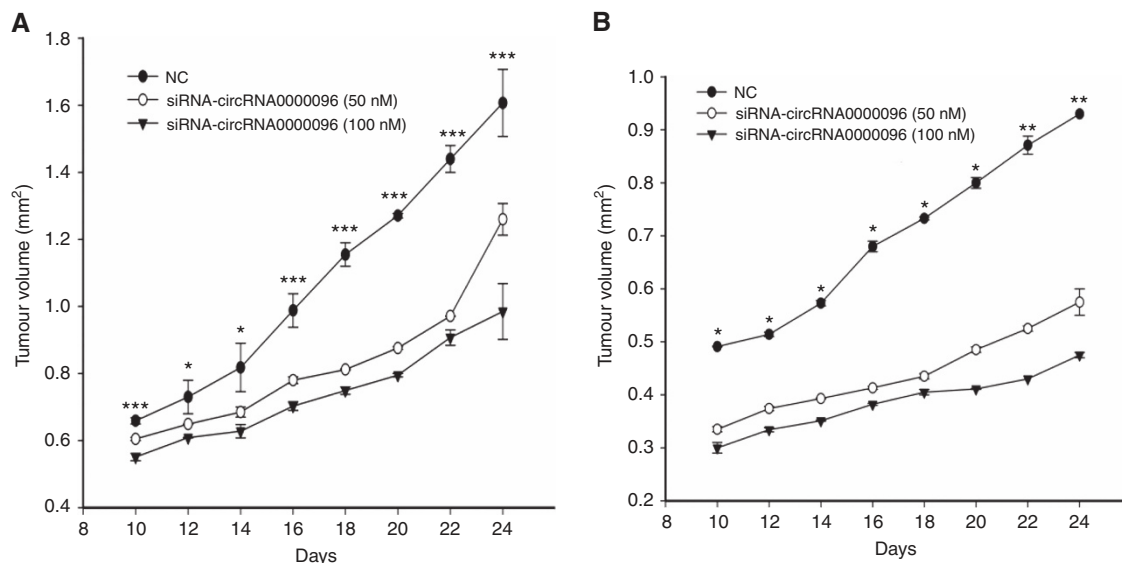

Figure 5. Transfection of siRNAs significantly inhibits tumour growth. The dose-dependent behaviour of hsa_circ_0000096 knockdown on BGC-823 (**A**) and MGC-803 (**B**) human gastric cancer cell lines. Data are presented as the mean ± s.d., $n = 3$. NC, negative control. *$P < 0.05$, **$P < 0.01$, ***$P < 0.001$.

western blotting to detect associated-protein levels. The results showed that when hsa_circ_0000096 was knocked down, the expression levels of cell cycle-related proteins cyclin D1 and CDK6 as well as migration-related proteins MMP-2 and MMP-9 were significantly decreased (Figure 4).

Xenograft nude mouse model experiments. The above results indicate the biological roles of hsa_circ_0000096 *in vitro*. Next, we used a xenograft nude mouse model to further study its functions. Two gastric cancer cell lines, BGC-823 and MGC-803, in which hsa_circ_0000096 was knocked down, were subcutaneously injected into nude mice. The results showed that transfection of siRNAs significantly inhibited tumour growth in a dose-dependent manner (Figure 5; Supplementary Figure 3). Then, we used a western blot analysis to detect the protein levels of cyclin D1, CDK6, MMP-2 and MMP-9; the results showed that all of these proteins were decreased (Figure 6).

IHC results. Immunohistochemical further found that the protein levels of cyclin D1, CDK6, MMP-2, MMP-9, Ki67 and VEGF were decreased in a dose-dependent manner; however, E-cadherin increased (Supplementary Figure 4).

DISCUSSION

In the past, circRNAs were considered to be the splicing error of transcripts (Grabowski *et al*, 1981; Capel *et al*, 1993; Braun *et al*, 1996; Pasman *et al*, 1996; Schindewolf *et al*, 1996; Zaphiropoulos 1996; Li and Lytton, 1999; Surono *et al*, 1999). However, with the wide applications of RNA sequencing, it was surprising to find that circRNAs were formed by nonlinear reverse splicing (Hansen *et al*, 2011; Salzman *et al*, 2012; Jeck *et al*, 2013; Memczak *et al*, 2013). Owing to this unique splicing, they are not easily degraded by RNase R. Thus, they could be more advantageous as molecular
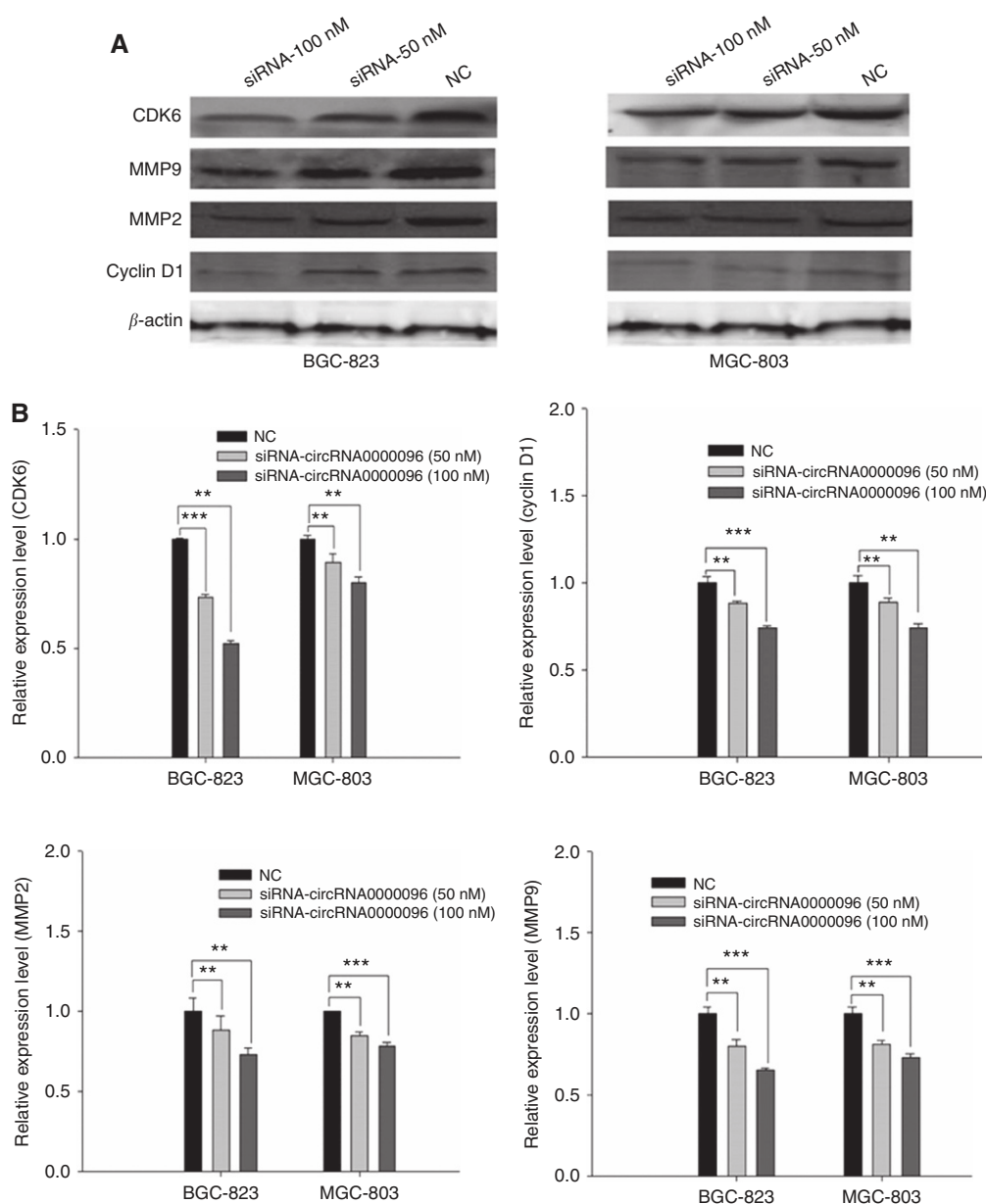

Figure 6. Knockdown of hsa_circ_0000096 suppresses cell cycle-related and migration-related protein expression. The results of cell cycle-related and migration-related protein levels in xenografts nude mouse models (**A**). Representative expression levels of cyclin D1, CDK6, MMP-2 and MMP-9 (**B**). Data are presented as the mean ± s.d., *n* = 3. NC, negative control. *$P < 0.05$, **$P < 0.01$, ***$P < 0.001$.

diagnostic markers. Our previous study has found that gastric cancer-associated circRNA002059 may represent a potential novel biomarker for the diagnosis of gastric cancer (Li *et al*, 2015). In this study, we first investigated the biological roles of hsa_circ_0000096.

Our study first revealed that hsa_circ_0000096 was down-regulated in gastric cancer tissues (Figure 1A) and gastric cancer cell lines (Figure 1B). Moreover, the AUC was 0.82 (Figure 1C). Furthermore, we found that low expression levels of hsa_circ_0000096 in gastric cancer were significantly associated with invasion and TNM stage (Supplementary Table 1). Through our *in vitro* experiments, we found that knockdown of hsa_circ_0000096 arrested cells at the G_0/G_1 phase (Supplementary Figure 1), and inhibited cell proliferation (Figure 2). The protein levels of CDK6, cyclin D1, MMP-2 and MMP-9 showed corresponding changes (Figure 4).

Through xenograft nude mouse models, we found that tumours grew slower after knockdown of hsa_circ_0000096 (Figure 5; Supplementary Figure 3). The protein levels of CDK6, cyclin D1, MMP-2, MMP-9, Ki67 and VEGF showed a dose-dependent decrease (Figure 6). The results of the IHC were consistent with those of the *in vitro* experiments (Supplementary Figure 4).

Generally, high expression of non-coding RNA in cancers might act as an oncogene, whereas low expressions of non-coding RNA act as a suppressor gene (Nie *et al*, 2012; Dang *et al*, 2015; Shen *et al*, 2015; Zhang *et al*, 2016). They directly or indirectly have an impact on tumour occurrence, development, metastasis and prognosis (Xie *et al*, 2014; Chen *et al*, 2015). However, our results were not consistent with these notions. This inconsistency may be explained by the use of competing endogenous RNA (ceRNA; Salmena *et al*, 2011).

Studies found that transcripts including mRNA, lncRNAs and circRNAs interacting with miRNAs have important roles in oncogenesis and cancer progression (Poliseno *et al*, 2010; Tay *et al*, 2011; Hou *et al*, 2014; Kumar *et al*, 2014; Ma *et al*, 2014; Rutnam *et al*, 2014). Hence, by using circRNA databases we first found that hsa_circ_0000096 may interact with 17 types of miRNA that could be used to form ceRNAs. Then, we selected two miRNAs, miR-200a and miR-224 to confirm their ceRNA relationship. The qRT–PCR results show that in GES-1, BGC-823, SGC-7901 and MGC-803 cells after knockdown of hsa_circ_0000096, the expression of miR-224 was decreased, whereas miR-200a was increased (Supplementary Figure 5). It has been reported that miR-224 (Mao *et al*, 2014) and miR-200a (Chang *et al*, 2015) have high and low expression in cancer tissues, respectively.

In conclusion, we found low expression levels of hsa_circ_0000096 in gastric cancer tissues and cell lines. hsa_circ_0000096 may become a potential novel biomarker for the diagnosis of gastric cancer. Moreover, hsa_circ_0000096 affected gastric cancer cell growth and migration by interfering with the expression of cell cycle-associated and migration-associated proteins.

ACKNOWLEDGEMENTS

CONFLICT OF INTEREST

The authors declare no conflict of interest.

REFERENCES

Braun S, Domdey H, Wiebauer K (1996) Inverse splicing of a discontinuous pre-mRNA intron generates a circular exon in a HeLa cell nuclear extract. *Nucleic Acids Res* **24**(21): 4152–4157.

Capel B, Swain A, Nicolis S, Hacker A, Walter M, Koopman P, Goodfellow P, Lovell-Badge R (1993) Circular transcripts of the testis-determining gene Sry in adult mouse testis. *Cell* **73**(5): 1019–1030.

Chang L, Guo F, Huo B, Lv Y, Wang Y, Liu W (2015) Expression and clinical significance of the microRNA-200 family in gastric cancer. *Oncol Lett* **9**(5): 2317–2324.

Chen WM, Huang MD, Kong R, Xu TP, Zhang EB, Xia R, Sun M (2015) Antisense long noncoding RNA HIF1A-AS2 is upregulated in gastric cancer and associated with poor prognosis. *Dig Dis Sci* **60**(6): 1655–1662.

Dang Y, Wang Y, Ouyang X, Wang L, Huang Q (2015) High expression of lncRNA-PCNA-AS1 in human gastric cancer and its clinical significances. *Clin Lab* **61**(11): 1679–1685.

Ghosal S, Das S, Sen R, Basak P, Chakrabarti J (2013) Circ2Traits: a comprehensive database for circular RNA potentially associated with disease and traits. *Front Genet* **4**: 283.

Glažar P, Papavasileiou P, Rajewsky N (2014) circBase: a database for circular RNAs. *RNA* **20**(11): 1666–1670.

Grabowski PJ, Zaug AJ, Cech TR (1981) The intervening sequence of the ribosomal RNA precursor is converted to a circular RNA in isolated nuclei of Tetrahymena. *Cell* **23**(2): 467–476.

Hansen TB, Jensen TI, Clausen BH, Bramsen JB, Finsen B, Damgaard CK, Kjems J (2013) Natural RNA circles function as efficient microRNA sponges. *Nature* **495**(7441): 384–388.

Hansen TB, Wiklund ED, Bramsen JB, Villadsen SB, Statham AL, Clark SJ, Kjems J (2011) miRNA-dependent gene silencing involving Ago2-mediated cleavage of a circular antisense RNA. *EMBO J* **30**(21): 4414–4422.

Hou P, Zhao Y, Li Z, Yao R, Ma M, Gao Y, Zhao L, Zhang Y, Huang B, Lu J (2014) LincRNA-ROR induces epithelial-to-mesenchymal transition and contributes to breast cancer tumorigenesis and metastasis. *Cell Death Dis* **5**: e1287.

Jeck WR, Sorrentino JA, Wang K, Slevin MK, Burd CE, Liu J, Marzluff WF, Sharpless NE (2013) Circular RNAs are abundant, conserved, and associated with ALU repeats. *RNA* **19**(2): 141–157.

Kumar MS, Armenteros-Monterroso E, East P, Chakravorty P, Matthews N, Winslow MM, Downward J (2014) HMGA2 functions as a competing endogenous RNA to promote lung cancer progression. *Nature* **505**(7482): 212–217.

Li P, Chen S, Chen H, Mo X, Li T, Shao Y, Xiao B, Guo J (2015) Using circular RNA as a novel type of biomarker in the screening of gastric cancer. *Clin Chim Acta* **444**: 132–136.

Li T, Mo X, Fu L, Xiao B, Guo J (2016) Molecular mechanisms of long noncoding RNAs on gastric cancer. *Oncotarget* **7**(8): 8601–8612.

Li XF, Lytton J (1999) A circularized sodium-calcium exchanger exon 2 transcript. *J Biol Chem* **274**(12): 8153–8160.

Ma MZ, Li CX, Zhang Y, Weng MZ, Zhang MD, Qin YY, Gong W, Quan ZW (2014) Long non-coding RNA HOTAIR, a c-Myc activated driver of malignancy, negatively regulates miRNA-130a in gallbladder cancer. *Mol Cancer* **13**: 156.

Mao S, He N, Xin L, Zeng F, Cao J (2014) Effect of antisense miR-224 on gastric cancer cell proliferation and apoptosis. *Zhonghua Zhong Liu Za Zhi* **36**(2): 2–96.

Memczak S, Jens M, Elefsinioti A, Torti F, Krueger J, Rybak A, Maier L, Mackowiak SD, Gregersen LH, Munschauer M, Loewer A, Ziebold U, Landthaler M, Kocks C, le Noble F, Rajewsky N (2013) Circular RNAs are a large class of animal RNAs with regulatory potency. *Nature* **495**(7441): 333–338.

Nie J, Liu L, Zheng W, Chen L, Wu Y, Du X, Du X, Han W (2012) microRNA-365, down-regulated in colon cancer, inhibits cell cycle progression and promotes apoptosis of colon cancer cells by probably targeting Cyclin D1 and Bcl-2. *Carcinogenesis* **33**(1): 220–225.

Pasman Z, Been MD, Garcia-Blanco MA (1996) Exon circularization in mammalian nuclear extracts. *RNA* **2**(6): 603–610.

Poliseno L, Salmena L, Zhang J, Carver B, Haveman WJ, Pandolfi PP (2010) A coding-independent function of gene and pseudogene mRNAs regulates tumour biology. *Nature* **465**(7301): 1033–1038.

Rutnam ZJ, Du WW, Yang W, Yang X, Yang BB (2014) The pseudogene TUSC2P promotes TUSC2 function by binding multiple microRNAs. *Nat Commun* **5**: 2914.

Salmena L, Poliseno L, Tay L, Kats L, Pandolfi PP (2011) A ceRNA hypothesis: the Rosetta Stone of a hidden RNA language? *Cell* **146**(3): 353–358.

Salzman J, Gawad C, Wang PL, Lacayo N, Brown PO (2012) Circular RNAs are the predominant transcript isoform from hundreds of human genes in diverse cell types. *PLos One* **7**(2): e30733.

Schindewolf C, Braun S, Domdey H (1996) In vitro generation of a circular exon from a linear pre-mRNA transcript. *Nucleic Acids Res* **24**(7): 1260–1266.

Shao Y, Ye M, Jiang X, Sun W, Ding X, Liu Z, Ye G, Zhang X, Xiao B, Guo J (2014) Gastric juice long noncoding RNA used as a tumor marker for screening gastric cancer. *Cancer* **120**(21): 3320–3328.

Shen R, Wang Y, Wang CX, Yin M, Liu HL, Chen JP, Han JQ, Wang WB (2015) MiRNA-155 mediates TAM resistance by modulating SOCS6-STAT3 signaling pathway in breast cancer. *Am J Transl Res* **7**(10): 2115–2126.

Surono A, Takeshima Y, Wibawa T, Ikezawa M, Nonaka I, Matsuo M (1999) Circular dystrophin RNAs consisting of exons that were skipped by alternative splicing. *Hum Mol Genet* **8**(3): 493–500.

Tay Y, Kats L, Salmens L, Weiss D, Tan SM, Ala U, Karreth F, Poliseno L, Provero P, Di Cunto F, Lieberman J, Rigoutsos I, Pandolfi PP (2011) Coding-independent regulation of the tumor suppressor PTEN by competing endogenous mRNAs. *Cell* **147**(2): 344–357.

Xia T, Chen S, Jiang Z, Shao Y, Jiang X, Li P, Xiao B, Guo J (2015) Long noncoding RNA FER1L4 suppresses cancer cell growth by acting as a competing endogenous RNA and regulating PTEN expression. *Sci Rep* **5**: 13445.

Xie X, Liu HT, Mei J, Ding FB, Xiao HB, Hu FQ, Hu R, Wang MS (2014) LncRNA HMlincRNA717 is down-regulated in non-small cell lung cancer and associated with poor prognosis. *Int J Clin Exp Pathol* **7**(12): 8881–8886.

Zaphiropoulos PG (1996) Circular RNAs from transcripts of the ratcytochrome P450 2C24 gene: correlation with exon skipping. *Proc Natl Acad Sci USA* **93**(13): 6536–6541.

Zhang G, Liu Z, Xu H, Yang Q (2016) miR-409-3p suppresses breast cancer cell growth and invasion by targeting Akt1. *Biochem Biophys Res Commun* **469**(2): 189–195.

Supplementary Information accompanies this paper on British Journal of Cancer website (http://www.nature.com/bjc)